Vol. 110: 213–225, 2014
doi: 10.3354/dao02754

DISEASES OF AQUATIC ORGANISMS
Dis Aquat Org

Published August 11

FREE ACCESS

Ameson metacarcini sp. nov. (Microsporidia) infecting the muscles of Dungeness crabs *Metacarcinus magister* from British Columbia, Canada

Hamish J. Small[1,*], Gary R. Meyer[2], Grant D. Stentiford[3], Jason S. Dunham[2], Kelly Bateman[3], Jeffrey D. Shields[1]

[1]Department of Environmental and Aquatic Animal Health, Virginia Institute of Marine Science, College of William & Mary, PO Box 1346, Gloucester Point, VA 23062, USA

[2]Department of Fisheries and Oceans, Pacific Biological Station, 3190 Hammond Bay Road, Nanaimo, BC V9T 6N7, Canada

[3]European Union Reference Laboratory for Crustacean Diseases, Centre for Environment, Fisheries, and Aquaculture Science (Cefas), Weymouth Laboratory, Dorset DT4 8UB, UK

ABSTRACT: The Dungeness crab *Metacarcinus magister* supports a large and valuable fishery along the west coast of North America. Since 1998, Dungeness crabs exhibiting pink- to orange-colored joints and opaque white musculature have been sporadically observed in low prevalence from the Fraser River delta of British Columbia, Canada. We provide histological, ultrastructural, and molecular evidence that this condition is caused by a new microsporidian parasite. Crabs displaying gross symptoms were confirmed to have heavy infections of ovoid-shaped microsporidian spores (~1.8 × 1.4 µm in size) within muscle bundles of the skeletal musculature. The parasite apparently infected the outer periphery of each muscle bundle, and then proliferated into the muscle fibres near the centre of each infected bundle. Light infections were observed in heart tissues, and occasionally spores were observed within the fixed phagocytes lining the blood vessels of the hepatopancreas. Transmission electron microscopy (TEM) revealed multiple life stages of a monokaryotic microsporidian parasite within the sarcoplasm of muscle fibres. Molecular analysis of partial small subunit rRNA sequence data from the new species revealed an affinity to *Ameson*, a genus of Microsporidia infecting marine crustaceans. Based on morphological and molecular data, the new species is distinct from *Nadelspora canceri*, a related microsporidian that also infects the muscles of this host. At present, little is known about the distribution, seasonality, and transmission of *A. metacarcini* in *M. magister*.

KEY WORDS: *Ameson* · Crab · Crustacea · Parasite · Microspora

INTRODUCTION

The Dungeness crab *Metacarcinus magister* supports large commercial fisheries and is harvested by commercial, First Nation, and recreational fishers along the west coast of North America from the Aleutian Islands, Alaska, to Point Conception, California (Pauley et al. 1989). In British Columbia (BC), Canada, the Fraser River delta in the Strait of Georgia is a highly productive habitat for Dungeness crab and supports the second largest commercial crab fishery there. Since 1998, Dungeness crabs exhibiting pink- to orange-colored joints and opaque white musculature have been sporadically observed from the Fraser River delta. In 2003, a preliminary investigation into the cause of the discolored musculature and joints revealed heavy infections of small ovoid spores resembling microsporidians (G. R. Meyer unpubl. data).

*Corresponding author: hamish@vims.edu

The Microsporidia comprise a phylum of spore-forming unicellular parasites that infect host groups from all major animal taxa in all environments (Canning & Vávra 2000, Smith 2009, Stentiford et al. 2013a). Recent phylogenetic assessments place them within the phylum Cryptomycota (James et al. 2013), but they have traditionally been placed in the kingdom Animalia as Microspora, or more recently in the kingdom Fungi (Lee et al. 2008). Microsporidians infect terrestrial hosts including humans, and beneficial and pest insects, but they are also frequently described from aquatic hosts where they can cause important diseases to commercial species. Of the 187 genera described to date, almost half are known to infect aquatic organisms (Stentiford et al. 2013a). The Microsporidia are considered to be one of the most common and pathogenic parasites of marine and freshwater crustaceans and parasitize all orders of Crustacea (Sparks 1985, Meyers 1990, Sindermann 1990, Morado 2011). However, only 11 to 12 recognized species use brachyuran crabs, and they are not well described or studied from these hosts.

Dungeness crabs are susceptible to a variety of infective agents including a *Chlamydia*-like organism (Sparks et al. 1985), a parasitic ciliate *Mesanophrys pugettensis* (Morado & Small 1994, Morado et al. 1999), a rarely encountered *Hematodinium*-like parasitic dinoflagellate (Meyers & Burton 2009), and an unusual microsporidian, *Nadelspora canceri* (Olson et al. 1994). The microsporidian *N. canceri* has unique needle-shaped spores and was originally described in Dungeness crabs from Alsea Bay, Oregon (Olson et al. 1994), and was later identified in Dungeness crabs from Bodega Bay, California, to Gray's Harbor, Washington (Childers et al. 1996). Prevalence of the parasite ranged from 0.4% in crabs from Gray's Harbor, Washington, to 41.2% in crabs from Tillamook Bay, Oregon. The only other known reports of microsporidian infections in Dungeness crabs is the brief mention of an undescribed species (family Nosematidae) in 2 conference abstracts (Morado & Sparks 1988a,b), the mention of a microsporidian separate from *N. canceri* infecting 3 of 1134 Dungeness crabs from Puget Sound, Washington, and Winchester Bay, Oregon (Childers et al. 1996), and the mention of an undescribed microsporidium causing 'pink crab' in a small percentage (<1%) of Dungeness crabs from Yaquina Bay, Oregon (www.dfw.state.or.us/MRP/shellfish/crab/research.asp).

As part of a routine stock assessment survey of the crabs from the Fraser River delta in 2011, samples of Dungeness crabs displaying discolored joints were collected for histology, electron microscopy, and nucleic acid analysis in an effort to further characterize the parasite. In this paper we provide field observations on prevalence, a histopathological description of the disease caused by this parasite, and use ultrastructural features, a proposed life cycle, and molecular phylogenetic analysis of a partial small subunit (SSU) rRNA sequence to describe a new microsporidian from the Dungeness crab *M. magister.*

MATERIALS AND METHODS

Sample collection

Dungeness crabs *Metacarcinus magister* were collected by standardized trap gear from the Fraser River delta, British Columbia, Canada (49° 05′ N, 123° 19′ W; Fig. 1), during spring and fall, 2011 to 2013. Fishing gear was circular commercial traps with stainless steel mesh and closed escape ports to retain smaller crabs. Trap mesh size generally precluded crabs smaller than approximately 120 mm carapace width (CW, longest width between epibranchial notches) from being vulnerable to research traps. Traps were baited with dead herring *Clupea pallasi* enclosed in a bait jar and deployed for approximately 24 h (overnight soak). Sampling depths ranged from 5 to 100 m. Crabs from each trap haul were examined for gross signs of infection (orange-colored joints; Fig. 2) and relevant biological information, including sex and carapace width were recorded. The potential sexual bias in prevalence was investigated using the Mantel-Haenszel chi-squared test with time (month and year) as strata. In October 2011, tissue samples from specimens show-

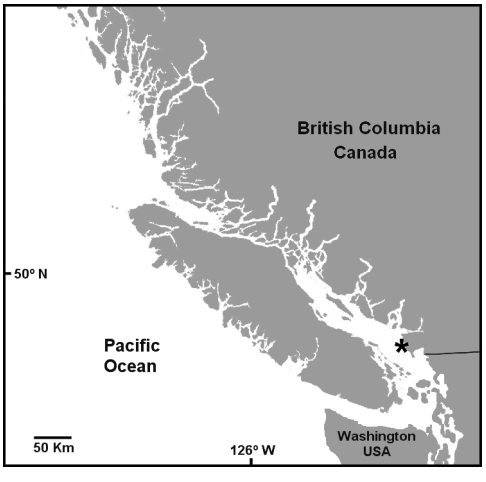

Fig. 1. British Columbia, Canada; the Fraser River delta study area is indicated with an asterisk

Fig. 2. The female Dungeness crab *Metacarcinus magister* on the left exhibits orange-colored joints, a typical gross sign of infection with *Ameson metacarcini* sp. nov., compared to a normal (uninfected) crab on the right

ing gross signs of infection were preserved for pathology, TEM, and DNA analyses.

Histopathology

Small pieces of the muscles, heart, gill, and hepatopancreas were excised from crabs displaying external signs of infection (Fig. 2) and fixed in Davidson's fixative (Howard et al. 2004), then processed using routine histological techniques. Tissue sections were cut at 5 µm and stained with Harris's modified haematoxylin and eosin (H&E), and a subset of sections was processed through modified Giemsa and Gram techniques (Howard et al. 2004). Histological slides were examined and photographed via light microscopy at 100 to 1000× magnification.

TEM

Small pieces of muscle and heart tissue (approximately 3 mm^3) were excised from crabs displaying external signs of infection (Fig. 2) and fixed in 2.5% glutaraldehyde in 0.1 M phosphate buffer at 4°C (for up to 25 d), and then rinsed 3 times in 0.1 M phosphate buffer. Fixed tissue samples were placed in 0.1 M sodium cacodylate buffer (pH 7.4) for transport to the Cefas Laboratory, Weymouth, UK. Fixed tissue samples were post-fixed for 1 h in 1.0% osmium tetroxide in 0.1 M sodium cacodylate buffer. Specimens were washed 3 times in 0.1 M sodium cacodylate buffer before dehydration through a graded acetone series. Specimens were embedded in Epoxy Resin 812 (Agar Scientific-pre-mix kit 812, Agar Scientific) and polymerized overnight at 60°C. Semithin (1 to 2 µm) sections were stained with Toluidine Blue for viewing with a light microscope to identify suitable target areas. Ultrathin sections (70 to 90 nm) of these areas were mounted on uncoated copper grids and stained with uranyl acetate and Reynolds' lead citrate (Reynolds 1963). Grids were examined using a JEOL JEM 1210 transmission electron microscope and digital images captured using a Gatan Erlangshen ES500W camera and Gatan Digital Micrograph™ software.

DNA extraction, SSU rRNA gene amplification, and sequencing

Muscle and heart tissue samples from infected crabs were preserved directly in 95% ethanol. Total DNA was isolated from preserved muscle tissues from 4 crabs infected with the microsporidian (3 from 2011 and 1 from 2003) using a modified protocol consisting of glass beads to rupture the parasite cysts prior to DNA isolation and recovery (see Stentiford et al. 2010). Briefly, samples of the ethanol-preserved microsporidian-infected muscle tissues (~1 to 2 mm^3) were placed in sterile deionized water to facilitate the removal of residual ethanol. The tissue samples were minced with a sterile scalpel blade, added to 300 µl buffer AE (Qiagen) with 0.3 g of 0.1 mm glass beads prior to disruption using a Fast Prep FP120 homogenizer (Thermo Savant) for 2 rounds of 30 s at full speed. The tubes were briefly centrifuged on a bench-top mini-centrifuge to sediment the glass beads and cell debris, and DNA was recovered from the supernatants using a Tissue Kit (Qiagen) following the manufacturer's recommendations. Also extracted by the same methods was an archived ethanol-preserved microsporidian-infected muscle sample from a single female Dungeness crab caught in February, 2003, from Sansum Narrows, British Columbia, Canada (48° 47′ N, 123° 33′ W). All extracted DNA samples were quantified using a NanoDrop 2000 spectrophotometer and stored at –20°C.

A fragment of the SSU rRNA gene from the microsporidian infecting the crabs was amplified from all 4 genomic DNA samples using previously described primers (Zhu et al. 1993): the forward primer V1 (5′-CAC CAG GTT GAT TCT GCC TGA C-3′) and the reverse primer 1492R (5′-GGT TAC CTT GTT ACG ACT T-3′). Each 20 µl reaction contained 10 mM Tris-HCl, pH 8.3, 50 mM KCl, 1.5 mM $MgCl_2$, 0.2 mM of each dNTP, 0.2 µM of each primer, 0.5 U of *Taq* polymerase (Applied Biosystems), and 1 µl genomic DNA

(100 to 140 ng μl^{-1}). Amplifications were performed with an initial denaturation temperature of 94°C for 5 min; followed by 40 cycles at 94°C for 1 min, 52°C for 1 min and 72°C for 2 min; with a final elongation step at 72°C for 5 min. Amplified products were visualized by agarose gel electrophoresis (1.5% w/v), stained with ethidium bromide, and viewed under an ultraviolet light source.

Amplification products of approximately 1300 bp were excised from agarose gels using a sterile scalpel blade and purified using a QIAquick Gel Extraction Kit (Qiagen). The purified amplification products were cloned into the plasmid pCR®4-TOPO® (Invitrogen) and transformed into competent *Escherichia coli* using a TOPO TA Cloning® Kit (Invitrogen) following the manufacturer's protocols. Transformed bacterial colonies were screened for inserts using a PCR-based screening reaction using the M13 primers included in the TOPO TA Cloning Kit. Aliquots of M13 amplification products containing the correct size insert were treated with shrimp alkaline phosphatase (SAP) and exonuclease I (*Exo* I) (Amersham Biosciences) prior to sequencing. PCR products were bi-directionally sequenced using the Big Dye Terminator kit (Applied Biosystems) with M13 sequencing primers and one-quarter of the recommended concentration of Big Dye. Aliquots of 10 µl of each sequencing reaction product were electrophoretically separated on an ABI 3130 Genetic Analyzer (Applied Biosystems). Three clones were bidirectionally sequenced for each sample.

Phylogenetic analysis

Forward and reverse sequencing reactions were imported into CodonCode Aligner (Version 3.7.1.1) for trimming of vector and primer sequences. Consensus sequences were aligned in MacVector (Version 12.5.1) and then subjected to Basic Local Alignment Search Tool (BLAST) searches of the National Center for Biotechnology (NCBI) database (www.ncbi.nlm.nih.gov). Partial SSU sequences from microsporidia with the highest similarity scores, as well as 22 others found infecting aquatic hosts, were downloaded from GenBank for inclusion in phylogenetic analyses. Multiple alignments of the microsporidian SSU sequences were performed using the CLUSTALW algorithm in MacVector 12.5.1 using the default gap settings for multiple and pairwise alignment. The full alignment was 1115 bp in length. Maximum-likelihood and neighbor-joining analyses were performed using MEGA 6 (Tamura et al. 2013). All models of evolution available in this sequence analysis package were independently assessed during maximum-likelihood analyses. The partial SSU sequence from *Thelohania solenopsae* (AF031538) was used as an outgroup. Robustness of trees was tested with 1000 bootstrap replicates. Genetic distance (uncorrected '*p*') calculations were performed using MEGA6 on an alignment of partial SSU sequences (898 bp in length) from *Ameson pulvis*, *A. michaelis*, and the microsporidian from *M. magister*.

RESULTS

Field observations

Dungeness crabs *Metacarcinus magister* with gross signs of infection (orange-colored joints and opaque, white muscles, see Fig. 2) were observed in 0.00 to 0.38% of the total catch (Table 1) from stock assessment surveys conducted in the Fraser River delta during the period from 2011 to 2013. While the overall number of infections was low (38 out of 27 782 crabs), the prevalence of infection showed a strong bias for females when controlled for time (month and year) of capture (Mantel-Haenszel chi-squared = 50.69, p = 0.00). No male crabs were infected, and the prevalence in females varied from 0.00 to 1.22% (Table 1). Infected females ranged in size from 107 to 150 mm CW and were caught at depths from 5 to 100 m. Infected crabs behaved similarly to normal crabs, with no apparent lethargy or signs of morbidity. Most infected crabs were collected where the main arm of the Fraser River empties into the Strait of Georgia. This area also produced the highest trap catches of females.

Table 1. Prevalence of gross signs of microsporidian infection among Dungeness crabs *Metacarcinus magister* caught by trap in the Fraser River delta, British Columbia, Canada. In brackets: number of individuals with gross signs of infection/total caught

Date	Female crabs (%)	Male crabs (%)	Total catch (%)
May 2011	0.15 (4/2699)	0.00 (0/2476)	0.08 (4/5175)
Oct 2011	0.55 (8/1455)	0.00 (0/1750)	0.25 (8/3205)
May 2012	0.18 (4/2209)	0.00 (0/3243)	0.07 (4/5452)
Oct 2012	0.69 (9/1302)	0.00 (0/2123)	0.26 (9/3425)
May 2013	0.00 (0/1826)	0.00 (0/3155)	0.00 (0/4981)
Oct 2013	1.22 (15/1230)	0.00 (0/2706)	0.38 (15/3936)

Prior to 2011, only 10 Dungeness crabs (6 males, 4 females) with colored joints were observed and recorded by fisheries biologists in the Fraser River delta. Five males were observed in 1998, and one in 2003; these crabs ranged in size from 132 to 172 mm CW and were collected at depths of 18 to 90 m. Four females were observed in 1998, 2003, and 2006, and they ranged in size from 128 to 142 mm CW and were collected from depths of 20 to 99 m.

Pathology and ultrastructure

Histological and wet mount smears of infected muscle from Dungeness crabs with gross signs of disease confirmed the presence of ovoid microsporidian spores (Fig. 3A,D). Although some staining variability was observed between specimens and tissue type, individual parasites were defined as Gram positive (blue to deep purple staining). The Gram staining technique was superior to both H&E and Giemsa for visualizing infections by histology, presumably because the former penetrated the exospore wall and did not decolorize with the destaining step.

Examination of histological tissue sections revealed heavy infection of the skeletal muscles. Infections were apparently initiated on the periphery of a muscle bundle, with lateral spread around the circumference of the bundle (Fig. 3B). In more advanced infections, all of the muscle fibres within the bundle were infected. Numerous spores were observed within the myocytes of the striated muscles (Fig. 3C); other developmental stages were difficult to discern via light microscopy. Degenerative and necrotic mussel bundles, heavily infected with spores, were commonly observed. Light infections were also observed in the heart myocytes where the spores had a tendency to stain deep purple rather than blue (Fig. 3D). Additionally, necrotic spores were occasionally observed in the hemal sinuses and clusters of fixed phagocytes lining the blood vessels of the hepatopancreas (Fig. 3E) and gills (Fig. 3F). Spores were likely released from ruptured muscle fibres and transported to these tissues via the hemolymph.

TEM revealed multiple life cycle stages of a monokaryotic microsporidian within the sarcoplasm of infected muscle fibres. The earliest stage observed was an apparent uninucleate meront (Fig. 4A), although a sectioning artefact may have masked the presence of a partner nucleus. Diplokaryons were likely formed by division of the uninucleate meront nucleus (Fig. 4B). Diplokaryotic meronts were surrounded by a simple cell membrane and appeared to undergo vacuolation as they matured (Fig. 4C). The transition to diplokarytic sporont was marked by thickening of the spore wall (Fig. 4D) and a further mitotic event in which each nucleus comprising the diplokaryon underwent division to create a quadranucleate sporont (Fig. 4E). The quadranucleate sporont developed into a chain-like form in which nuclei became isolated, and associated with a distinct perinuclear vacuole (Fig. 4F). At this stage, the quadranucleate spore wall remained thick, but precursors of the spore extrusion apparatus (e.g. polar filament and anchoring disk) had not yet formed within each developing sporoblast.

Ultrastructurally, sporoblasts were distinguished from sporonts by the formation of precursors of the spore extrusion apparatus in close association with isolated nuclei and their peripheral vacuole (Fig. 5A). This apparatus formed prior to the separation of individual sporoblasts from the quadranucleate sporont (Fig. 5B). Eventual cytokinesis of the sporoblasts coincided with coiling of the polar filament at the periphery of the sporoblast cytoplasm and the formation of the anchoring disk (Fig. 5C). Maturation of liberated uninucleate sporoblasts into spores was characterized by elongation of the spore wall, centralization of the monokaryotic nucleus, peripheral coiling of the polar filament, terminal positioning of the anchoring disk, and formation of a laminar polaroplast between the anchoring disk and the nucleus (Fig. 5D). Fully developed spores measured approximately 1.8 × 1.4 µm and possessed a trilaminar wall consisting of a plasma membrane, a thick electron-lucent endospore, and a thinner electron-dense exospore. The isofilar polar filament had 9 to 12 turns, 8 to 9 of which form a linear outer coil, and the remainder occupy a position towards the centre of the spore. The polar filament culminated in a manubrial region that passed through the laminar polaroplast to a terminal anchoring disk (Fig. 5E–G). Mature spores possessed hair-like appendages projecting from the exospore into the surrounding sarcoplasm (Fig. 6). All observed life-cycle stages occurred in direct contact with the muscle sarcoplasm.

Molecular phylogeny

All partial SSU gene sequences generated from the 2003 and 2011 samples were 1232 bp in length (after removal of primer sequences), and all were identical. BLAST analysis of this SSU fragment indicated an affinity to microsporidia-infecting crustaceans, with *Nadelspora canceri* from *M. magister* and *Ameson*

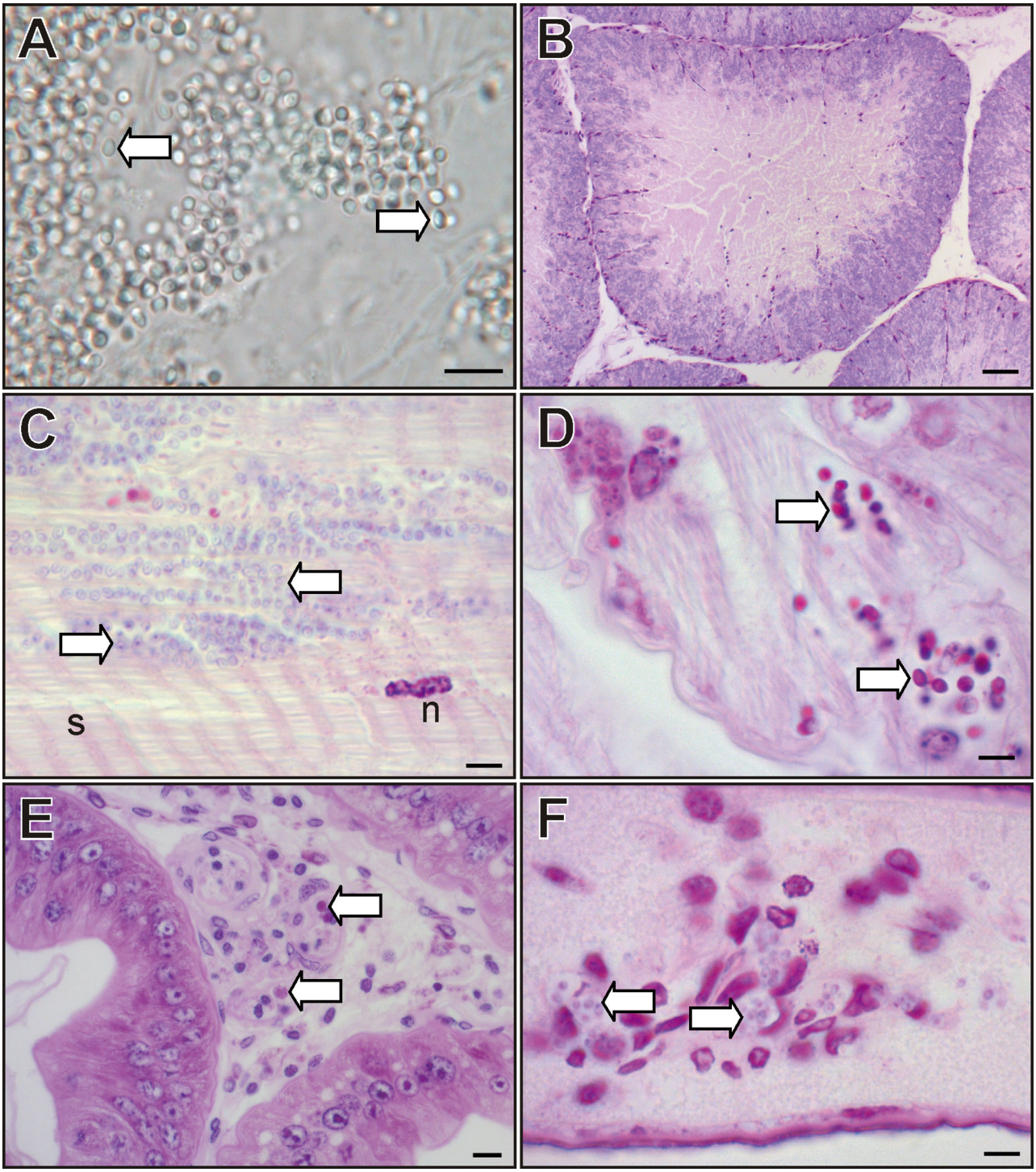

Fig. 3. Light microscopy of *Ameson metacarcini* sp. nov. infecting *Metacarcinus magister*. (A) Muscle smear showing numerous ovoid shaped spores (arrows), phase contrast. Scale bar = 5 µm. (B–F) Histological tissue sections with Gram stain. (B) Transverse section through skeletal musculature showing heavy infection of spores in the peripheral regions of a muscle bundle (blue staining area) with an uninfected or lightly infected central area (pink). Scale bar = 50 µm. (C) Longitudinal section through striated (s) muscle showing numerous spores (arrows) and myocyte nucleus (n). Scale bar = 5 µm. (D) Heart muscle showing spores (arrows) that stain deep purple instead of blue. Note that these spores are ovoid in shape. Scale bar = 3 µm. (E) Spores in the fixed phagocytes of the arterioles in the hepatopancreas. The fixed phagocytes have been activated and appear to be phagocytizing the spores (arrows). Scale bar = 10 µm. (F) Necrotic spores in the vascular spaces of the gills (arrows). Scale bar = 5 µm.

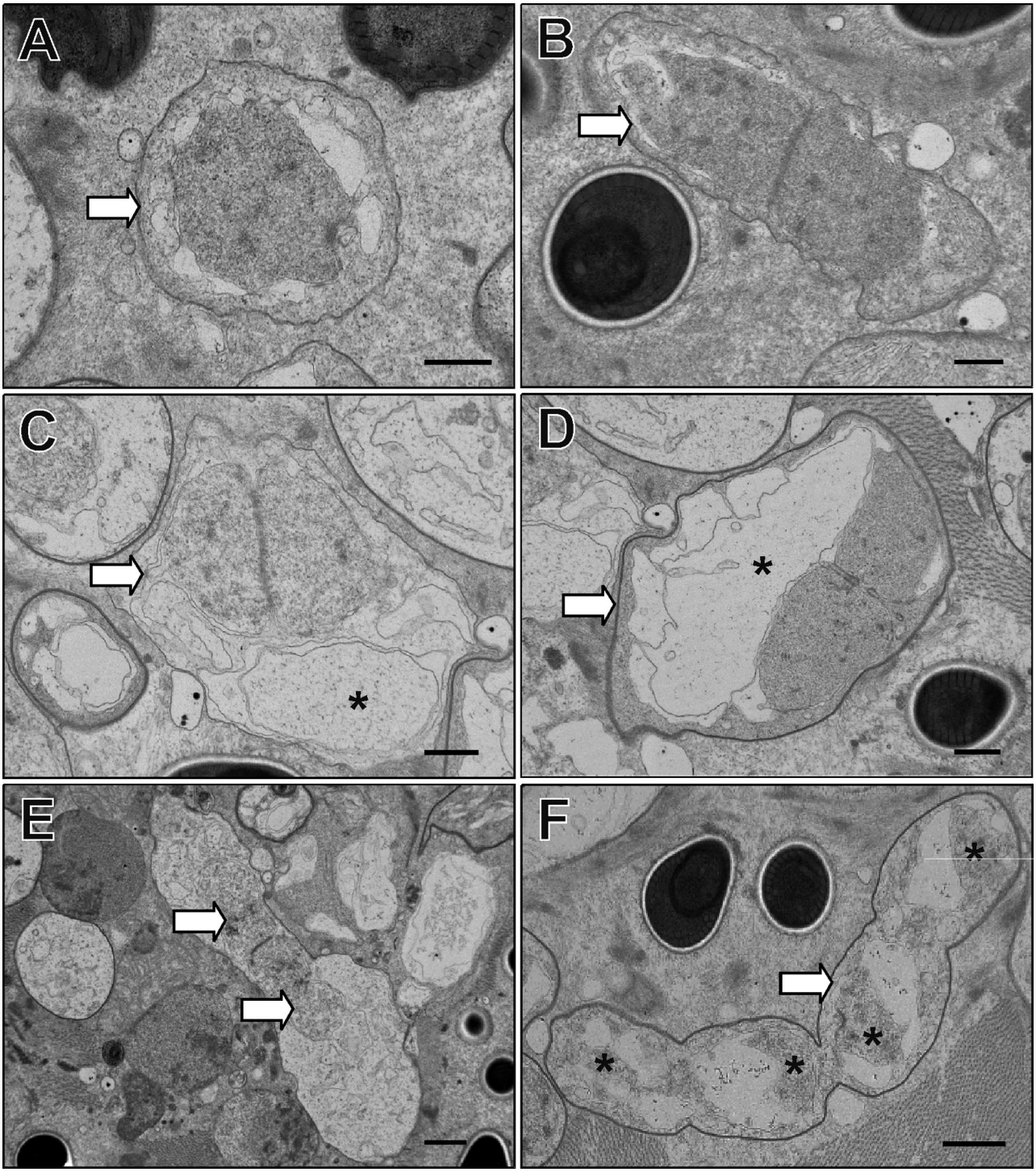

Fig. 4. Transmission electron microscopy of meronts and early sporogony in *Ameson metacarcini* sp. nov. infecting the muscles of *Metacarcinus magister*. (A) Uninucleate meront (arrow). Scale bar = 500 nm. (B) Diplokaryotic meront (arrow). Scale bar = 500 nm. (C) Diplokaryotic meront (arrow) with vacuolated cytoplasm (asterisk). Scale bar = 500 nm. (D) Diplokaryotic sporont with relatively electron-dense membrane forming (arrow) and highly vacuolated cytoplasm (asterisk). Scale bar = 500 nm. (E) Diplokaryotic sporont in the process of nuclear division (arrows) to form a quadranucleate sporont. Scale bar = 1 µm. (F) Tetranucleate sporont chain (arrow) containing 4 single nuclei (asterisks) prior to the formation of spore extrusion precursors. Scale bar = 1 µm

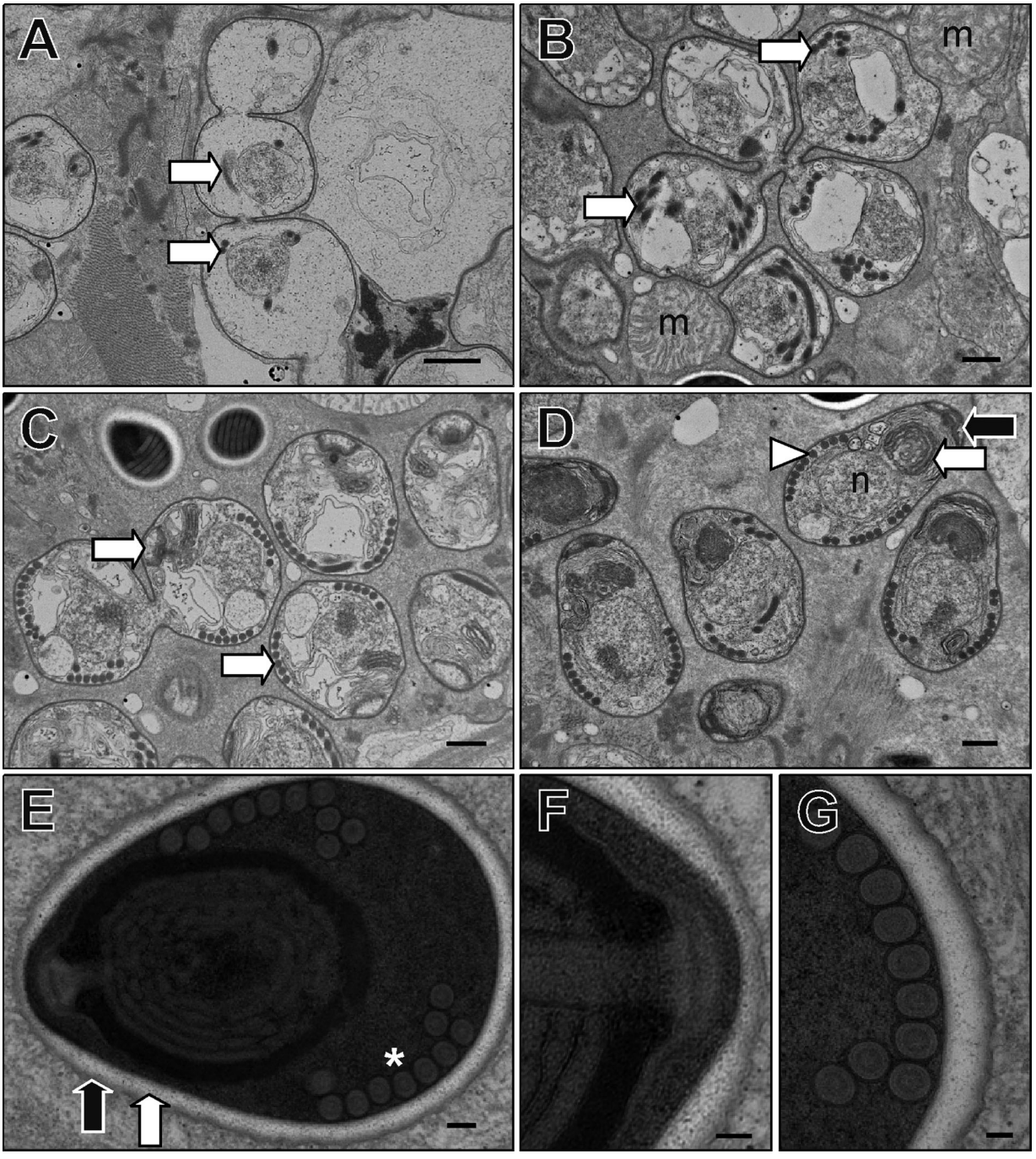

Fig. 5. Transmission electron microscopy of late-stage sporogony in *Ameson metacarcini* sp. nov. infecting the muscles of *Metacarcinus magister*. (A) Late tetranucleate sporont chain with early development of spore extrusion precursors (arrows). Scale bar = 1 µm. (B) Budding of uninucleate pre-sporoblasts from quadranucleate sporont. Spore extrusion precursors, such as the nascent polar tube, are clearly visible (arrows). Parasites lie in close contact with host cell mitochondria (m). Scale bar = 500 nm. (C) Liberation and early development of sporobasts. Spore extrusion precursors migrate to approximate positions observed within the mature spore (arrows). Scale bar = 500 nm. (D) Sporoblasts become increasingly electron dense and contain a visible polaroplast (white arrow), an anchoring disk (black arrow), peripheral arrangement of polar filament coils (arrowhead), and a single nucleus (n). Scale bar = 500 nm. (E) Mature spore. Similar cellular arrangement to the late sporoblast but containing approximately 10 turns of the polar filament (asterisk), laminar polaroplast, an electron-dense cytoplasm, and a trilaminar spore wall comprised of an inner plasmalemma, a thick electron lucent endospore (white arrow), and a thin electron-dense exospore (black arrow). Scale bar = 100 nm. (F) Detail of terminal anchoring disk of mature spore. Scale bar = 100 nm. (G) Detail of coiled isofilar polar filament in mature spore. Scale bar = 50 nm

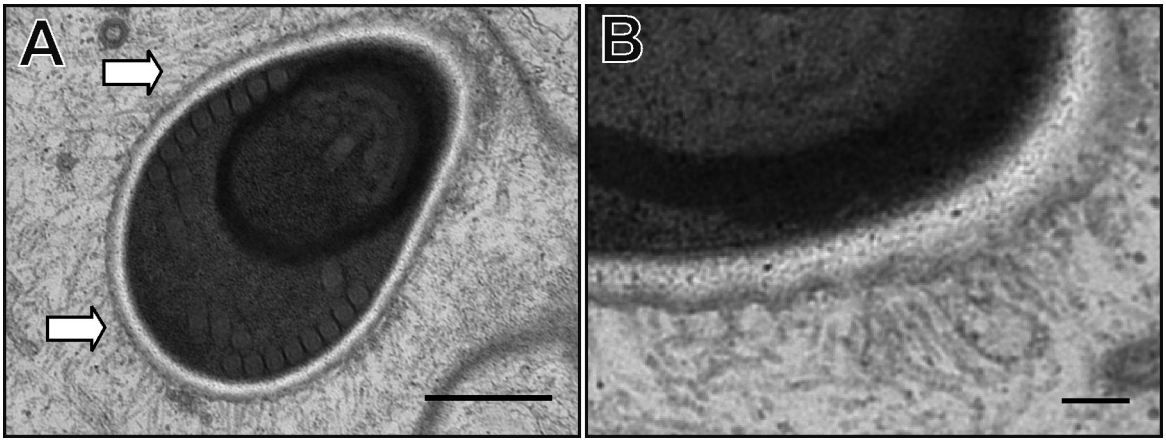

Fig. 6. Mature spore of *Ameson metacarcini* sp. nov. showing (A) bristle-like appendages (white arrows) on the exospore surface. Scale bar = 500 nm. (B) Increased magnification of bristle-like appendages. Scale bar = 100 nm

pulvis from *Carcinus maenas* having the highest maximum identity scores (both 95%). All maximum likelihood (Fig. 7) and neighbor-joining (data not shown) analyses produced similar tree topologies and confirmed a close affiliation among other species of *Ameson*, placing the microsporidian from *M. magister* within a highly supported (100%) clade containing *A. michaelis*, *A. pulvis*, and *N. canceri*. Genetic distances between the microsporidian from *M. magister* and *A. pulvis* ('*p*' = 0.047) and *A. michaelis* ('*p*' = 0.060) were comparable to that observed between *A. pulvis* and *A. michaelis* ('*p*' = 0.040). The partial SSU rRNA gene sequences obtained from the microsporidian-infecting *M. magister* were deposited in GenBank with Accession Numbers KJ652546 to KJ652549. We used ultrastructural and phylogenetic data to erect a new species within the genus *Ameson*.

Taxonomic summary

Type species: *Ameson metacarcini* sp. nov.

Description: Parasite stages infecting the skeletal and heart muscles of a marine crustacean host. Spores ovoid, monokaryotic, approximately 1.8 × 1.4 µm in size in tissues fixed for TEM; in direct contact with muscle sarcoplasm of infected host cells. Polar filament with 9 to 12 coils, the majority forming a linear outer coil and the remainder occupying a position towards the centre of the spore. The observed life cycle progresses from an apparent uninucleate meront to diplokaryotic meront, quadranucleate meront, chain-like quadranucleate sporont, with cytokinesis to produce individual sporoblasts which develop into spores.

Type host: *Metacarcinus magister* (Dana, 1852)

Type locality: Fraser River delta (5 to 100 m depth), British Columbia, Canada.

Site of infection: Sarcoplasm of skeletal myofibrils, rarely in cardiac muscles, fixed phagocytes of hemal vessels.

Etymology: The specific name refers to its infection in the crab host *Metacarcinus magister*.

Type material: Syntype specimens of stained histological sections have been deposited with the Canadian Museum of Nature, Ottawa, Canada. TEM resin blocks have been deposited in the Registry of Aquatic Pathogens (RAP) at the Cefas Weymouth Laboratory, UK. The partial SSU rRNA gene sequences obtained from *A. metacarcini* have been deposited in GenBank with Accession Numbers KJ652546 to KJ652549.

DISCUSSION

Histological, ultrastructural, and molecular data were used to describe a new microsporidian, *Ameson metacarcini*, infecting Dungeness crabs, *Metacarcinus magister*, from British Columbia. Electron microscopy revealed developmental features of a monokaryotic microsporidian that are consistent with members of the genus *Ameson*. Likewise, phylogenetic analyses of a partial sequence of the SSU rRNA gene grouped *A. metacarcini* beside, but distinct, from *A. michaelis*, *A. pulvis*, and *Nadelspora canceri* previously described from marine crabs *Callinectes sapidus*, *Carcinus maenas*, and *M. magister*, respectively.

The putative earliest stages infecting muscle bundles of *M. magister* were apparently uninucleate, or mono-

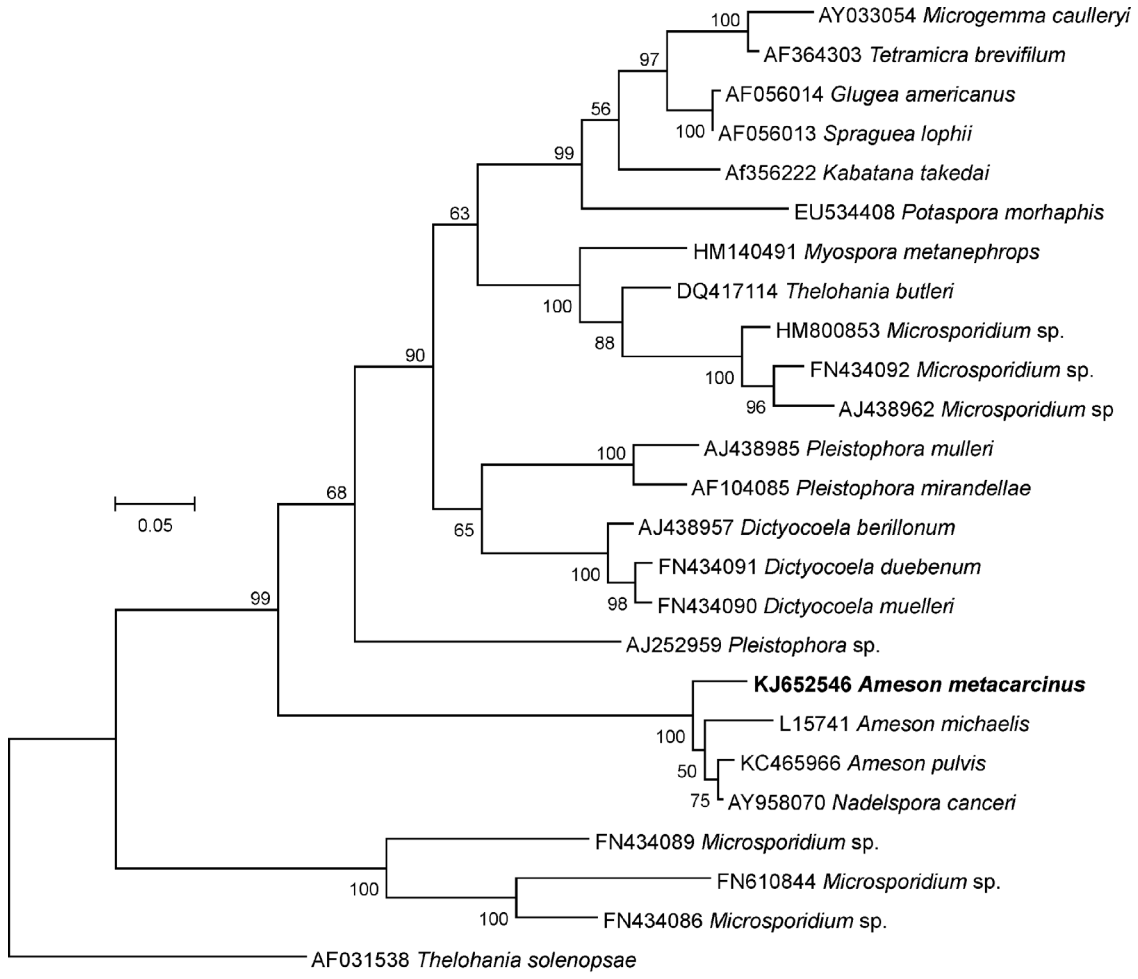

Fig. 7. Maximum-likelihood tree resulting from analysis of the small subunit rRNA gene sequence from *Ameson metacarcini* sp. nov. (in bold) and other aquatic microsporidia. *Thelohania solenopsae* was used as the outgroup. This analysis was performed using the Tamura-Nei model of evolution within MEGA 6. Numbers at nodes represent bootstrap support values for each clade

karyotic meronts. Binucleate (diplokaryotic) meronts showed remarkable similarity to stages observed in *A. atlanticum* infecting *Cancer pagurus*, *A. pulvis* infecting *C. maenas*, and *A. michaelis* infecting *C. sapidus* (Weidner 1970, Vivarès & Sprague 1979, Vivarès & Azevedo 1988, Sprague 1965, Stentiford et al. 2013b). Meronts underwent vacuolation, thickening of the parasite spore wall, and a decrease in the nuclear:cytoplasm ratio as they progressed to become the chain-forming quadranucleate sporonts that are characteristic of the genus. Precursors of the spore extrusion apparatus were observed in sporoblasts prior to their separation from the sporont.

Morphologically, *A. metacarcini* can be tentatively distinguished from other species in the genus by the size of the fully developed spore (Table 2). The spores are most similar in size to those reported from *A. atlanticum* (1.8 × 1.4 µm vs. 2.0 × 1.5 µm); however, the latter species was described from a different host (*C. pagurus*) from the French Atlantic coastline. Few other morphological characters appear to be useful, and these characters are generally comparable to other reported but undescribed species in the genus (Shields & Wood 1991, Kiryu et al. 2009, Ryazanova & Eliseikina 2010). Spores of *A. metacarcini* had hair-like villous projections that have previously been observed in other *Ameson* species (Vivarès & Sprague 1979, Vivarès & Azevedo 1988, Kiryu et al. 2009, Ryazanova & Eliseikina 2010, Stentiford et al. 2013b). Vivarès & Azevedo (1988) used the projections on the spore to separate the genera *Ameson* from *Perezi* within the family Pereziidae (see also Canning & Vávra 2000). The role of these organelles is still unknown, though Vávra et al.

Table 2. Comparison of spore characteristics for different species of *Ameson* described from decapods

Species	Spore size (µm)	Spore projections	Polar tube	Reference
A. michaelis	2.2 × 1.7 (live, light microscopy)			Sprague (1965)
	1.7 × 1.2 (stained, light microscopy)			Sprague (1965)
	1.6 × 1.2 (electron microscopy)		11 coils	Sprague et al. (1968)
A. pulvis	1.3 × 1.0 (electron microscopy)	Short basal and long terminal portion	8 coils	Vivarès & Sprague (1979)
	1.2 × 1.0 (electron microscopy)	Villous projections	8–9 coils	Stentiford et al. (2013b)
A. atlanticum	2.0 × 1.5 (electron microscopy)	Long, bipartite	11–12 coils	Vivarès & Azevedo (1988)
A. metacarcini	1.8 × 1.4 (electron microscopy)	Long bristle-like appendages	9–12 coils	Present study

(1981) suggested that they may aid dispersal of the released spore stage in aquatic environments and Lom & Corliss (1967) conjectured that they may be involved in transporting metabolites from the host to the parasite.

Phylogenetic data confirmed our ultrastructural observations of an affiliation of *A. metacarcini* within the genus *Ameson* as it placed with 100% support within a clade containing *A. michaelis*, *A. pulvis*, and *N. canceri*. Genetic distances between *A. metacarcini* and previously described *Ameson* species (for which there is molecular sequence data available) were similar to those observed between previously described species, further supporting the new species proposal. The inclusion of *N. canceri* within a clade containing species of *Ameson*, at least based upon SSU rRNA sequences, is surprising as it has a diplokaryotic lineage and produces elongated, needle-like spores, and would seem to be at odds with conventional taxonomy using morphological features. However, Stentiford et al. (2013b) recently observed morphological plasticity in a microsporidian (presumed to be *A. pulvis*) infecting the marine crab *C. maenas*. Those authors observed *A. pulvis* having 2 spore morphologies based on their location within host tissues and state of infection. The needle-like spores, similar to *N. canceri* from *M. metacarcini*, occurred early in infections and primarily in cardiac muscles, whereas the ovoid *Ameson*-like spores, with pronounced surface projections, occurred later in infections and primarily in skeletal muscles (Stentiford et al. 2013b). In histological assessments of infected *M. metacarcini* muscles, heart, gill, and hepatopancreas tissues we did not observe elongated needle-like spores resembling *N. canceri* in either early or advanced infections. Olson et al. (1994) in the original description of *N. canceri* only encountered needle-like spore forms infecting *M. metacarcini*. However, in a subsequent study, 3 of 1134 *M. metacarcini* infected with microsporidia were found to harbor a microsporidian with ovoid spores morphologically dissimilar to *N. canceri* (Childers et al. 1996). Recent studies combining ecological, morphological, and molecular data have demonstrated significant plasticity in morphological features within certain taxa (Vossbrinck & Debrunner-Vossbrinck 2005, Stentiford et al. 2010, 2013b). Indeed, some genera of microsporidians change their spore characteristics with temperature, switching between free spores and octospores within a sporophorous vesicle depending on environmental temperature (e.g. Maddox & Sprenkel 1978, Jouvenaz & Lofgren 1984). Thus, additional studies should now include a combination of morphological and molecular data to investigate plasticity in the life cycles of these parasites.

At present the geographic distribution of *A. metacarcini* in Dungeness crabs from British Columbia remains essentially unknown. The 2003 sample included in our molecular analysis was from a female Dungeness crab captured from Sansum Narrows, which is located between Vancouver Island and Saltspring Island, approximately 40 km from the Fraser River delta. Aside from confirming its presence in Dungeness crabs from these 2 sample locations in British Columbia, and in Canada, for at least 10 yr, gross clinical signs similar to those described above (exhibiting pink- to orange-colored joints) have only been reported in Dungeness crabs from Yaquina Bay, Oregon, USA (Oregon Department of Fish and Wildlife, ODFW). As staff from ODFW were also identifying *N. canceri* infections based on different gross signs of infection, and given that these 2 pathogens are the only microsporidia known to infect Dungeness crabs, it is possible that the crabs from Oregon may have been infected with *A. metacarcini*. If confirmed, the known range of this parasite may extend throughout the range of its host species. Because of the pathological nature of the parasite, future studies aimed at documenting its distribution and impacts may be warranted.

Due to gear selectivity that limited retention of crabs smaller than ~120 mm CW, the prevalence in juvenile Dungeness crabs is unknown, yet pathogens are often most prevalent in and damaging to early juvenile stages in crustacean populations (Bateman et al. 2011, Shields 2012). Likewise, the prevalence of *A. metacarcini* in crabs that do not display pathognomonic signs of infection is unknown. Discoloration of host carapace, arthroidal membranes, and hemolymph and tissues are macroscopic signs of late-stage/patent infections in many crustaceans (e.g. Field et al. 1992, Shields & Behringer 2004, Stentiford et al. 2010), and use of gross visual assessment methods may significantly underestimate the actual prevalence of *A. metacarcini* in trapped Dungeness crabs, as has been observed in snow crabs macroscopically diagnosed with *Hematodinium* infections (Pestal et al. 2003). In addition, it is somewhat surprising that crabs possessing advanced infections were able to enter traps as parasite loads in muscle tissues were considerable, and in some cases heavy infections essentially replaced infected muscle tissues. We speculate there may be additional infected individuals too weak to enter baited traps. Future assessments using trawl-platforms that provide non-selective sampling may provide a more realistic approach to estimating the prevalence of *A. metacarcini* in Dungeness crab populations.

In contrast to Childers et al. (1996) who found that *N. canceri* was 3 times more likely to infect male Dungeness crabs compared to females, we only observed gross signs of microsporidian infection (orange-colored joints) in female crabs from spring and fall assessments during the period from 2011 to 2013 and in the single sample from 2003. Prior to the current study, gross signs of infection were observed in 5 male crabs captured in 1998; however, the presence of microsporidia was not confirmed microscopically. Few studies have considered sexual differences in the prevalence levels in microsporidian infections in decapod hosts. Of the limited number that have, prevalence levels were reported as approximately equal between host sexes (Parsons & Khan 1986, Herbert 1988, Skurdal et al. 1990, Ryazanova & Eliseikina 2010). However, sexual differences are known from microsporidian infections in amphipod hosts where the parasites are known to be transmitted vertically (e.g. Bulnheim & Vávra 1968, Terry et al. 2004, Haine et al. 2007). In crabs, potential factors for sexual differences may include behavioural differences, stresses imposed by reproduction, or hormonal differences between sexes.

Acknowledgements. The following people assisted in collecting and sampling Dungeness crabs: fisheries staff Georg Jorgensen, Sarah Davies, and Sandra Bassett, and the Canadian Coast Guard crew of the CCGV 'Neocaligus'. H.J.S. and J.D.S. were supported by NSF EID Grant OCE 0723662. G.D.S. and K.B. were supported by grants from the European Commission (#C5839) and UK Department for Environment, Food and Rural Affairs (#FB002) (both to G.D.S.). This paper is Contribution No. 3364 of the Virginia Institute of Marine Science, College of William & Mary.

LITERATURE CITED

Bateman KS, Hicks RJ, Stentiford GD (2011) Disease profiles differ between populations of pre-recruit and recruit edible crabs (*Cancer pagurus*) from a major commercial fishery. ICES J Mar Sci 68:2044–2052

Bulnheim HP, Vávra J (1968) Infection by microsporidian *Oetosporea effeminans* sp. n., and its sex determining influence in the amphipod *Gammuflls daebeni.* J Parasitol 54:241–248

Canning EU, Vávra J (2000) Phylum Microsporida. In: Lee JL, Leedale GF, Bradbury P (eds) The illustrated guide to the Protozoa, 2nd edn. Society for Protozoologists, Allen Press, Lawrence, KS, p 39–126

Childers RK, Reno PW, Olson RE (1996) Prevalence and geographic range of *Nadelspora canceri* (Microspora) in Dungeness crab *Cancer magister.* Dis Aquat Org 24: 135–142

Field RH, Chapman CJ, Taylor AC, Neil DM, Vickerman K (1992) Infection of the Norway lobster *Nephrops norvegicus* by a *Hematodinium*-like species of dinoflagellate on the West Coast of Scotland. Dis Aquat Org 13: 1–15

Haine ER, Motreuil S, Rigaud T (2007) Infection by a vertically transmitted microsporidian parasite is associated with a female-biased sex ratio and survival advantage in the amphipod *Gammarus roeseli.* Parasitology 134: 1363–1367

Herbert BW (1988) Infection of *Cherax quadricarinatus* (Decapoda: Parastacidae) by the microsporidian *Thelohania* sp. (Microsporidia: Nosematidae). J Fish Dis 11: 301–308

Howard DW, Lewis EJ, Keller BJ, Smith CS (2004) Histological techniques for marine bivalve molluscs and crustaceans, 2nd edn. NOAA Tech Memo NOS NCCOS 5

James TY, Pelin A, Bonen L, Ahrendt S, Sain D, Corradi N, Stajich JE (2013) Shared signatures of parasitism and phylogenomics unite the Cryptomycota and Microsporidia. Curr Biol 23:1548–1553

Jouvenaz DP, Lofgren CS (1984) Temperature-dependent spore dimorphism in *Burenella dimorpha* (Microspora: Microsporida). J Protozool 31:175–177

Kiryu Y, Behringer DC, Landsberg JH, Petty BD (2009) Microsporidiosis in the Caribbean spiny lobster *Panulirus argus* from southeastern Florida, USA. Dis Aquat Org 84:237–242

Lee SC, Corradi N, Byrnes EJ, Torres-Martinez S, Dietrich FS, Keeling PJ, Heitman J (2008) Microsporidia evolved from ancestral sexual fungi. Curr Biol 18:1675–1679

Lom J, Corliss JO (1967) Ultrastructural observations on the development of the microsporidian protozoon *Plistophora hyphessobryconis* Schaperclaus. J Eukaryot Microbiol 14:141–152

Maddox J, Sprenkel RK (1978) Some enigmatic species of the genus *Nosema.* Misc Publ Entomol Soc Am 11: 65–84

Meyers TR (1990) Diseases caused by protistans and metazoans. In: Kinne O (ed) Diseases of marine animals, Vol 3. Biologische Anstalt Helgoland, Hamburg, p 350–389

Meyers TR, Burton T (2009) Diseases of wild and cultured shellfish in Alaska. Alaska Department of Fish & Game, Anchorage, AK

Morado JF (2011) Protistan diseases of commercially important crabs: a review. J Invertebr Pathol 106:27–53

Morado FJ, Small EB (1994) Morphology and stomatogenesis of *Mesanophrys pugettensis* n. sp. (Scuticociliatida: Orchitphryidae), a facultative parasitic ciliate of the Dungeness crab, *Cancer magister* (Crustacea: Decapoda). Trans Am Microsc Soc 113:343–364

Morado JF, Sparks AK (1988a) A review of infectious diseases of the Dungeness crab, *Cancer magister.* In: Proceedings of the annual meeting of the National Shellfisheries Association. J Shellfish Res 7:127 (Abstract)

Morado JF, Sparks AK (1988b) Infectious diseases of the Dungeness crab, *Cancer magister.* In: American Fisheries Society International Fish Health Conference Handbook. AFS, Bethesda, MD, p 16 (Abstract)

Morado JF, Giesecke RH, Syrjala SE (1999) Molt related mortalities of the Dungeness crab *Cancer magister* caused by a marine facultative ciliate *Mesanophrys pugettensis.* Dis Aquat Org 38:143–150

Olson RE, Tiekotter KL, Reno PW (1994) *Nadelspora canceri* n. g., n. sp., an unusual microsporidian parasite of the Dungeness crab, *Cancer magister.* J Eukaryot Microbiol 41:349–359

Parsons DG, Khan RA (1986) Microsporidiosis in northern shrimp, *Pandalus borealis.* J Invertebr Pathol 47:74–81

Pauley GB, Armstrong DK, Van Citter R, Thomas GL 1989 Species profiles: life histories and environmental requirements of coastal fishes and invertebrates (Pacific Southwest) — Dungeness crab. US Fish Wildl Serv Biol Rep 82(11.121). US Army Corps of Engineers, TR EL-82-4

Pestal GP, Taylor DM, Hoenig JM, Shields JD, Pickavance R (2003) Monitoring the prevalence of the parasitic dinoflagellate *Hematodinium* sp. in snow crabs *Chionoecetes opilio* from Conception Bay, Newfoundland. Dis Aquat Org 53:67–75

Reynolds ES (1963) The use of lead citrate at high pH as an electron-opaque stain in electron microscopy. J Cell Biol 17:208–212

Ryazanova TV, Eliseikina MG (2010) Microsporidia of the genera *Thelohania* (Thelohaniidae) and *Ameson* (Perezidae) in two species of lithodid crabs from the Sea of Okhotsk. Russ J Mar Biol 36:435–442

Shields JD (2012) The impact of pathogens on exploited populations of decapod crustaceans. J Invertebr Pathol 110:211–224

Shields JD, Behringer DC Jr (2004) A new pathogenic virus in the Caribbean spiny lobster *Panulirus argus* from the Florida Keys. Dis Aquat Org 59:109–118

Shields JD, Wood FEI (1991) Pathology and fine structure of *Ameson* sp. a microsporidian from the blue sand crab *Portunus pelagicus.* Mem Queensl Mus 31:403

Sindermann CJ (1990) Principal diseases of marine fish and shellfish, Vol 2: Diseases of marine shellfish, 2nd edn. Academic Press, New York, NY, p 93–144

Skurdal J, Qvenild T, Taugbøl T, Fjeld E (1990) A 6-year study of *Thelohania contejeani* parasitism of the noble crayfish, *Astacus astacus* L., in Lake Steinsfjorden, S.E. Norway. J Fish Dis 13:411–415

Smith JE (2009) The ecology and evolution of microsporidian parasites. Parasitology 136:1901–1914

Sparks AK (1985) Protozoan diseases. In: Sparks AK (ed) Synopsis of invertebrate pathology exclusive of insects. Elsevier Science Publishing, Amsterdam, p 239–309

Sparks AK, Morado JF, Hawkes JW (1985) A systemic microbial disease in the Dungeness crab, *Cancer magister*, caused by a *Chlamydia*-like organism. J Invertebr Pathol 45:204–217

Sprague V (1965) *Nosema* sp. (Microsporidia, Nosematidae) in the musculature of the crab *Callinectes sapidus.* J Protozool 12:66–70

Sprague V, Vernick SH, Lloyd BJ (1968) The fine structure of *Nosema* sp. Sprague, 1965 (Microsporidia, Nosematidae) with particular reference to stages in sporogony. J Invertebr Pathol 12:105–117

Stentiford GD, Bateman KS, Small HJ, Moss J, Shields JD, Reece KS, Tuck I (2010) *Myospora metanephrops* (n. gn., n. sp.) from marine lobsters and a proposal for erection of a new order and family (Crustaceacida; Myosporidae) in the Class Marinosporidia (Phylum Microspora). Int J Parasitol 40:1433–1446

Stentiford GD, Feist SW, Stone DM, Bateman KS, Dunn AM (2013a) Microsporidia: diverse, dynamic, and emergent pathogens in aquatic systems. Trends Parasitol 29: 567–578

Stentiford GD, Bateman KS, Feist SW, Chambers E, Stone DM (2013b) Plastic parasites: extreme dimorphism creates a taxonomic conundrum in the phylum Microsporidia. Int J Parasitol 43:339–352

Tamura K, Stecher G, Peterson D, Filipski A, Kumar S (2013) MEGA6: Molecular Evolutionary Genetics Analysis Version 6.0. Mol Biol Evol 30:2725–2729

Terry RS, Smith JE, Sharpe RG, Rigaud T and others (2004) Widespread vertical transmission and associated host sex-ratio distortion within the eukaryotic phylum Microspora. Proc R Soc Lond B Biol Sci 271:1783–1789

Vávra J, Barker RJ, Vivarès CP (1981) A scanning electron microscopic study of a microsporidian with a pansporoblast: *Thelohania maenadis.* J Invertebr Pathol 37:47–53

Vivarès CP, Azevedo C (1988) Ultrastructural observations of the life cycle of *Ameson atlanticum* sp. nov., a microsporidian parasitizing *Cancer pagurus* L. J Fish Dis 11: 379–387

Vivarès CP, Sprague V (1979) The fine structure of *Ameson pulvis* (Microspora, Microsporida) and its implications regarding classification and chromosome cycle. J Invertebr Pathol 33:40–52

Vossbrinck CR, Debrunner-Vossbrinck BA (2005) Molecular phylogeny of the Microsporidia: ecological, ultrastructural and taxonomic considerations. Folia Parasitol 52: 131–142

Weidner E (1970) Ultrastructural study of microsporidian development. I. *Nosema* sp. Sprague, 1965 in *Callinectes sapidus* Rathbun. Z Zellforsch 105:33–54

Zhu X, Wittner M, Tanowitz HB, Kotler D, Cali A, Weiss LM (1993) Small subunit rRNA sequence of *Enterocytozoon bieneusi* and its potential diagnostic role with use of the polymerase chain reaction. J Infect Dis 168:1570–1575

Editorial responsibility: Dieter Steinhagen, Hannover, Germany

Submitted: January 28, 2014; Accepted: April 17, 2014
Proofs received from author(s): July 10, 2014